

# Research on distance measurement method based on micro-accelerometer

Cite as: AIP Advances 11, 055126 (2021); <https://doi.org/10.1063/5.0054463>

Submitted: 19 April 2021 • Accepted: 10 May 2021 • Published Online: 24 May 2021

 Yonglei Shi, Liqing Fang, Deqing Guo, et al.



View Online



Export Citation



CrossMark

## ARTICLES YOU MAY BE INTERESTED IN

[Entropy generation minimization in bio-convective flow of nanofluid with activation energy and gyrotactic micro-organisms](#)

AIP Advances 11, 055017 (2021); <https://doi.org/10.1063/5.0047567>

[Design and analysis of shoulder joint exoskeleton rehabilitation mechanism based on gear and rack transmission](#)

AIP Advances 11, 055122 (2021); <https://doi.org/10.1063/5.0051484>

[A machine learning method for hardware Trojan detection on real chips](#)

AIP Advances 11, 055006 (2021); <https://doi.org/10.1063/5.0038773>

Call For Papers!

AIP Advances

SPECIAL TOPIC: Advances in  
Low Dimensional and 2D Materials

# Research on distance measurement method based on micro-accelerometer

Cite as: AIP Advances 11, 055126 (2021); doi: 10.1063/5.0054463

Submitted: 19 April 2021 • Accepted: 10 May 2021 •

Published Online: 24 May 2021



View Online



Export Citation



CrossMark

Yonglei Shi,<sup>1,2,a)</sup> Liqing Fang,<sup>1</sup> Deqing Guo,<sup>1</sup> Ziyuan Qi,<sup>1</sup> Jinye Wang,<sup>2</sup> and Jinli Che<sup>1</sup>

## AFFILIATIONS

<sup>1</sup> Army Engineering University of PLA, Shijiazhuang 050003, China

<sup>2</sup> School of Mechanical Engineering, Hebei University of Science and Technology, Shijiazhuang 050018, China

<sup>a)</sup> Author to whom correspondence should be addressed: [sylhbkd@hebust.edu.cn](mailto:sylhbkd@hebust.edu.cn)

## ABSTRACT

Limited by some engineering occasions and displacement sensors, it is usually difficult to measure the distance of moving objects directly. However, the acceleration of the moving object is usually easy to measure, so the distance of the moving object can be easily obtained through the acceleration integral. To solve this problem, a distance measurement system based on the micro-electro-mechanical system accelerometer is designed. The hardware structure of the system includes the data measurement module, data acquisition module, and data processing module. Thanks to the excellent characteristics of the sensor, the system can be used in a small space, overload impact, and other harsh environments. In this paper, a time domain algorithm based on acceleration integration is proposed. The algorithm not only has no loss of sampling points but also has cubic algebraic accuracy. The fixed output error caused by the installation position of the sensor is analyzed. The analysis shows that the error will lead to a serious trend error. For this problem, an algorithm for removing the trend term error is given. Aiming at the random zero drift of the sensor, the Kalman filter algorithm is used to reduce noise. The distance measurement experiment is carried out on the horizontal slide rail, and the calculation results show that the average measurement accuracy of this distance measurement system can reach 97.89%. The experimental results show the feasibility of the system and the validity of the data processing algorithm. The accuracy of the distance measurement system can meet most of the engineering needs, so it has important significance in the field of engineering distance measurement.

© 2021 Author(s). All article content, except where otherwise noted, is licensed under a Creative Commons Attribution (CC BY) license (<http://creativecommons.org/licenses/by/4.0/>). <https://doi.org/10.1063/5.0054463>

## I. INTRODUCTION

The technology of distance measurement based on acceleration has a long history. It has been widely used and developed in the fields of building health detection, micro-displacement measurement of roads and bridges, inertial navigation, and so on.<sup>1–3</sup> As early as in the 1960s, Berg proposed that there was a very simple transformation relationship among acceleration, velocity, and displacement signals at each point in the motion process of an object.<sup>4</sup> After the acceleration signal was obtained, velocity or displacement signals could be obtained by means of integration.<sup>5,6</sup> Therefore, the distance measurement technology based on acceleration is used to measure the ground deformation and the vibration velocity and displacement of other structures during earthquakes. The French railway tracks are equipped with an accelerometer and seismographs at various depths underground. In the study of the

railway vibration law, the researchers first filter the signal obtained by the acceleration sensor and then determine the boundary conditions. The vibration displacement of railway under load conditions is obtained by integrating the discrete acceleration signal in the time domain.

In the development of scientific theory and practical engineering applications, people have been trying to accurately measure velocity and displacement. Many related measurement theories and techniques have been developed and good results have been achieved in the distance measurement, for example, a non-contact laser rangefinder based on the transverse photoelectric effect. By modulating and demodulating the optical signal, it filters out the interference of the clutter signal and obtains the precise position signal of the illumination place. Another example is the radio fuze based on the Doppler effect, which emits electromagnetic waves to the target and receives the echo signal returned by the target.<sup>7</sup>

However, these distance measurement methods have great limitations. They depend too much on the reflection signal of the external object and need the interaction of the signal to realize the distance measurement.<sup>8,9</sup> However, in the actual application environment, the transmitted wave will be affected not only by the propagation medium but also by electromagnetic interference, weather, and other factors.<sup>10,11</sup> The most important thing is that there is no object to reflect the signal or no target reference point, which directly leads to the failure of such methods.

In order to deal with the problem of distance measurement, a method of displacement measurement without reference is proposed. In order to improve the accuracy and intelligence of distance measurement, a distance measurement system based on the MEMS (Micro-Electro-Mechanical system) accelerometer is designed.

The system can measure the acceleration of moving objects in real time and solve the moving distance in real time by using a digital signal processor (DSP). Through the program setting, the system can send out a specific signal at the predetermined moving distance, which improves the intelligence of the system. The MEMS accelerometer is a revolutionary new technology, which is widely used in medical, military, aerospace, and other fields.<sup>12-14</sup> Its main features are small size, high accuracy, and a simple interface circuit. Because the MEMS accelerometer can work normally under the impact of 200 000g, the measuring system can adapt to the impact overload environment. The small size of the MEMS accelerometer allows it to adapt to moving objects with tight internal spaces. The MEMS accelerometer outputs digital signals directly, so the interface circuit does not need to add A/D modules. In addition, the system has strong anti-interference capability. Thanks to the excellent characteristics of the MEMS accelerometer, the measuring system has a wide range of applications.

The MEMS acceleration sensor usually has zero drift and output error.<sup>15-17</sup> In order to obtain high ranging accuracy, the acceleration signal collected by the MEMS accelerometer must be processed effectively. Because the performance parameters and related indices of different types of sensors are greatly different, the measurement results are obviously different. On the basis of the hardware structure design, the problems of fixed output error and random zero drift of the MEMS acceleration sensor are treated by the related algorithm. The distance calculated from the processed acceleration data is of high precision.

## II. MEASUREMENT SYSTEM DESIGN

The system consists of a MEMS accelerometer, a DSP microprocessor, a power supply module, and a peripheral circuit. The overall framework of the system is shown in Fig. 1, which mainly includes the system control module, measurement module, and data reading module.

### A. System control module design

The control module adopts the DSP microprocessor. It mainly includes the data acquisition module, data processing module, and data storage module. The main work of the DSP microprocessor is the acquisition, calculation, and storage of acceleration. The DSP

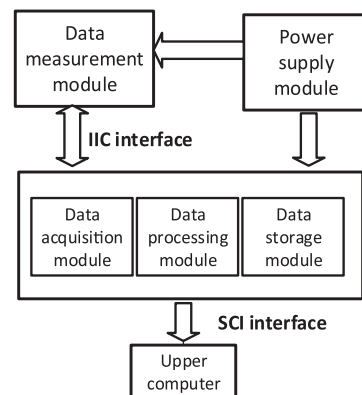


**FIG. 1.** Structure of the measurement system.

microprocessor has a floating-point operation unit and an independent multiplier. It adopts the advanced Harvard bus structure, which makes its program space and data space independent. Based on the above advantages, the DSP microprocessor has powerful data operation and processing ability. Its data processing ability and efficiency are much higher than those of single chip microcomputers, programmable logic controller (PLC), and other microprocessors, which ensure the system's fluency. Therefore, the DSP microprocessor can process and control the acceleration signal accurately in real time.

### B. System measurement module design

The MEMS accelerometer can measure the acceleration of a moving object in real time, and its external pin is very simple. It provides the IIC serial bus, which includes the clock line SCL and the data line SDA. In addition, VDD and GND are the power supply pins of the MEMS accelerometer. The structure and external pins of the MEMS accelerometer are shown in Fig. 2. In order to maintain the stability of the data transmission process, the clock line and the data line are connected with a pull resistor.

The MEMS accelerometer outputs digital signals in the form of binary complement, so there is no need for an analog-digital conversion circuit, which makes the whole circuit system relatively

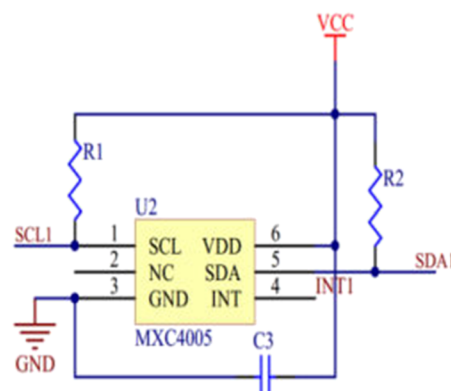


**FIG. 2.** External pin and interface circuit of the MEMS accelerometer.

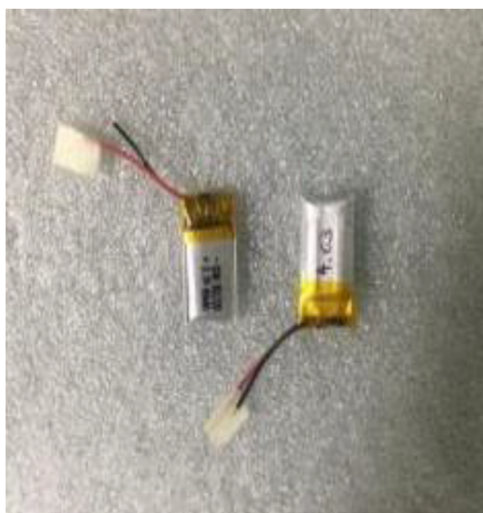


**FIG. 3.** The power supply of the system.

simple. Therefore, the reliability and communication efficiency in the process of system operation are improved.

### C. Design of the system data reading module

The MEMS accelerometer communicates with the DSP microprocessor through the serial communication interface IIC. After the system works normally, the MEMS accelerometer can measure the acceleration of the moving object in real time. The DSP microprocessor collects the acceleration from the MEMS accelerometer register in real time. The DSP microprocessor processes the acquired acceleration and stores the processing results in its internal serial FLASH. The data collected by the DSP microprocessor are transmitted to the master computer through its serial communication interface (SCI) for data analysis. Since universal serial bus (USB) interface

is widely used in computers, a serial port conversion chip SP3232 is needed in order to communicate between the DSP microprocessor and the computer. The chip converts the transistor-transistor logic (TTL) serial port signal of the DSP microprocessor into the RS232 serial port signal of the computer. As the core of the power supply module, the battery supplies power to the DSP microprocessor, MEMS accelerometer, and peripheral circuit, as shown in Fig. 3. The rated voltage of the battery is 3.7–4.2 V, which can be recharged several times, and the total storage capacity is not less than 55 mAh. The battery has excellent performance of small volume and high overload resistance, which can meet the experimental requirements. Each module is connected to form a complete hardware measurement system. The actual printed circuit is shown in Fig. 4.

### III. STATIC ACCURACY TEST OF THE SYSTEM

In order to verify the accuracy of acceleration signal acquisition, the static test of the acceleration signal was carried out for the measurement and control module when the system circuit board was completed. In order to verify the accuracy of the acquisition acceleration of the system, a gravitational field flip test was designed. The connected circuit board is fixed to a horizontal platform, and then, it is flipped  $0^\circ$ ,  $30^\circ$ ,  $60^\circ$ ,  $90^\circ$ ,  $210^\circ$ ,  $240^\circ$ , and  $270^\circ$ . In the test process, the x and y axes of the sensor were taken as the rotation axes to test, and the output accuracy of the sensor in two directions was verified successively. After the measurement is completed, the data in the memory will be read from the top computer to analyze the measurement accuracy. Two groups of data were arbitrarily selected, and MATLAB was used to draw the graph line. Acceleration points collected from seven angles were plotted together, and 100 points were selected from each angle, as shown in Fig. 5. The average test accuracy is shown in Table I.

According to the static test results, the circuit connection of the measurement system is stable and reliable, which can realize the acquisition, measurement, and processing of acceleration. The results of the gravity field inversion experiment and the average measurement accuracy show that the average measurement accuracy of acceleration is higher. However, when the MEMS accelerometer is in a static position, the accelerometer curve is not a straight line. This is caused by the random zero drift of the sensor. Further processing is needed to improve the measurement accuracy.

### IV. DISTANCE DETERMINATION ALGORITHM AND ERROR CONTROL ALGORITHM

#### A. Distance calculation algorithm based on acceleration

Since the MEMS accelerometer sampling interval is a constant value  $\Delta t$ , the acquired acceleration values are discrete.

The distance can be obtained by numerical integration of acceleration. Assume that the discrete acceleration signals collected by the sensor are  $a_0, a_1, a_2, \dots, a_{i-1}, a_i, a_{i+1}, \dots$ . The corresponding time points of each acceleration value are  $t_0, t_1, t_2, \dots, t_{i-1}, t_i, t_{i+1}, \dots$ , respectively.

The moving window method is used to intercept three adjacent sampling points, in turn, as a group. The three acceleration

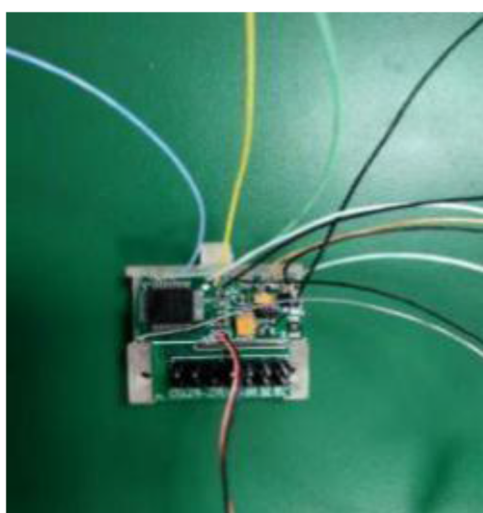


**FIG. 4.** Printed circuit boards for measuring systems.

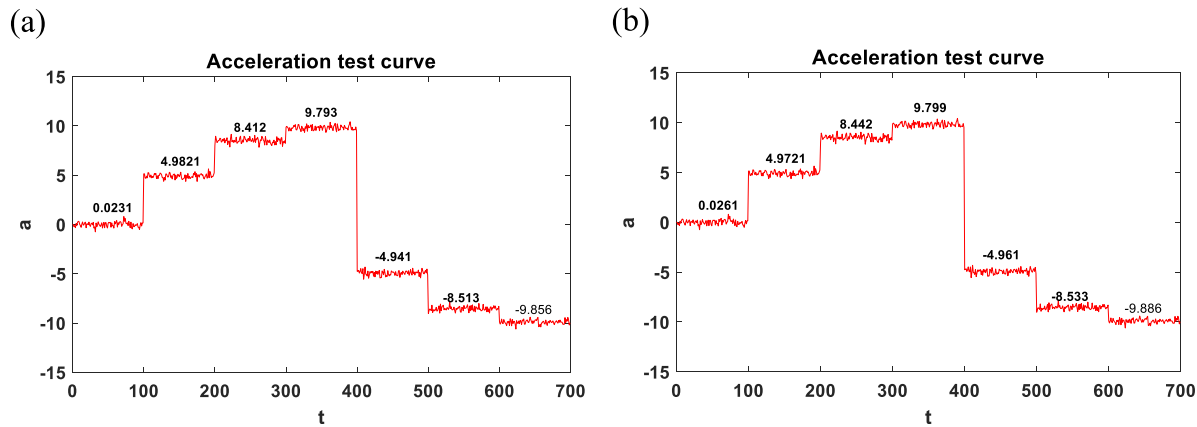


**FIG. 5.** Gravity field flip test results: (a) output of the x axis with the y axis as the rotation axis and (b) output of the y axis with the x axis as the rotation axis.

**TABLE I.** Average test accuracy.

Group	1	2	3	4	5
Average error ( $\text{m/s}^2$ )	0.0343	0.0378	0.0314	0.0415	0.0336

points in each moving window can be constructed as a quadratic function by Lagrange interpolation. Sliding rectangular windows are shown in Fig. 6. By calculating the definite integral of the quadratic function at the first two time points in the rectangular box, the velocity increment of the first two time points can be obtained. Sliding the rectangular window in turn, the velocity increment between any two adjacent acceleration points can be obtained by the same method. The following is the derivation of this algorithm.

Suppose that the three points in the sliding window at a certain moment are  $(t_{i-1}, a_{i-1})$ ,  $(t_i, a_i)$ , and  $(t_{i+1}, a_{i+1})$ . A quadratic function can be obtained by Lagrange interpolation as follows:

$$a = \frac{(t - t_i)(t - t_{i+1})}{(t_{i-1} - t_i)(t_{i-1} - t_{i+1})} a_{i-1} + \frac{(t - t_{i-1})(t - t_{i+1})}{(t_i - t_{i-1})(t_i - t_{i+1})} a_i + \frac{(t - t_{i-1})(t - t_i)}{(t_{i+1} - t_i)(t_{i+1} - t_{i-1})} a_{i+1}. \quad (1)$$

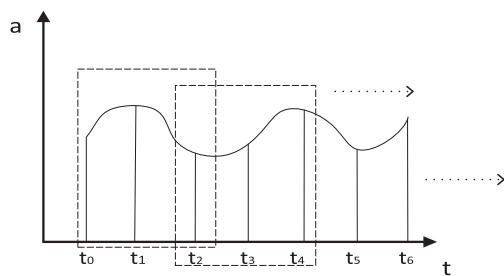


**FIG. 6.** Sliding window movement diagram.

Since the sampling interval of the sensor is fixed,  $\Delta t = t_{i+1} - t_i = t_i - t_{i-1}$ . Therefore, the above equation can be changed into

$$a = \frac{(t - t_i)(t - t_{i+1})}{2\Delta t^2} a_{i-1} - \frac{(t - t_{i-1})(t - t_{i+1})}{\Delta t^2} a_i + \frac{(t - t_{i-1})(t - t_i)}{2\Delta t^2} a_{i+1}. \quad (2)$$

Through deformation, the above equation can be changed into

$$a = \frac{a_{i-1} - 2a_i + a_{i+1}}{2\Delta t^2} t^2 + \frac{-3a_{i-1} + 4a_i - a_{i+1}}{2\Delta t} t + a_{i-1}. \quad (3)$$

By calculating the definite integral of the quadratic function between  $t_{i-1}$  and  $t_i$ , the velocity increment in this time period can be obtained as follows:

$$\Delta v_i = \int_{t_{i-1}}^{t_i} a \cdot dt = \frac{5a_{i-1} + 8a_i - a_{i+1}}{12} \Delta t. \quad (4)$$

The velocity  $v_n$  at any time can be obtained by accumulating the velocity increment  $\Delta v_i$  as follows:

$$v_n = v_0 + \sum_{i=1}^n \Delta v_i \quad (n = 1, 2, 3, \dots), \quad (5)$$

where  $v_0$  is the initial velocity and  $v_n$  is the velocity at any time. After the discrete velocity sequence is obtained from the discrete acceleration, the distance increment between adjacent sampling points and the moving distance at any time can be obtained by using the same method.

The distance increment from  $t_{i-1}$  to  $t_i$  can be obtained as follows:

$$\Delta s_i = \int_{t_{i-1}}^{t_i} v dt = \frac{5v_{i-1} + 8v_i - v_{i+1}}{12} \Delta t. \quad (6)$$

The movement distance at any time can be obtained by adding displacement increments as follows:

$$s_n = s_0 + \sum_{i=1}^n \Delta s_i \quad (n = 1, 2, 3, \dots). \quad (7)$$

It can be seen from the above derivation that the algorithm fully considers the smooth and continuous characteristics between discrete acceleration points.

The algorithm has cubic algebraic accuracy and does not lose the number of sampling points in the integration process. The method has relatively high precision in solving the moving distance. In addition, the algorithm is easy to program and is very suitable for numerical integration of discrete acceleration.

## B. Kalman filter algorithm to remove random drift

The output value of the MEMS accelerometer usually has the characteristic of random drift. Random drift means that in any state, the sensor will output an error value that changes with time. This random variable value will cause a certain error in the acceleration signal output by the sensor. Figure 7 shows the random output of the acceleration signal of the sensor in a static state. Multiple static tests show that the mean value of the random output signal of the MEMS acceleration sensor is about 0 and the variance is a fixed value. This kind of random noise signal is often called Gaussian white noise.

The Kalman filter algorithm is the most widely used and direct method to deal with such random noise and interference signals.<sup>18–20</sup> The principle of Kalman filtering technology is to use the data of the previous time to predict the current data and then get the optimal estimate of the current time. This algorithm cyclically updates the state estimate for the next moment. Suppose that the state equation and observation equation of the discrete system are

$$X_{k|k-1} = FX_{k-1} + BU_k + \omega_k, \quad (8)$$

$$Z_k = H_k X_k + v_k, \quad (9)$$

where  $F$  is the state transition matrix,  $H_k$  is the system measurement matrix,  $\omega_k$  is the estimation deviation of the system,  $v_k$  is the system measurement noise, and  $BU_k$  is the system control quantity. The premise of the Kalman filter is that  $\omega_k$  and  $v_k$  are independent

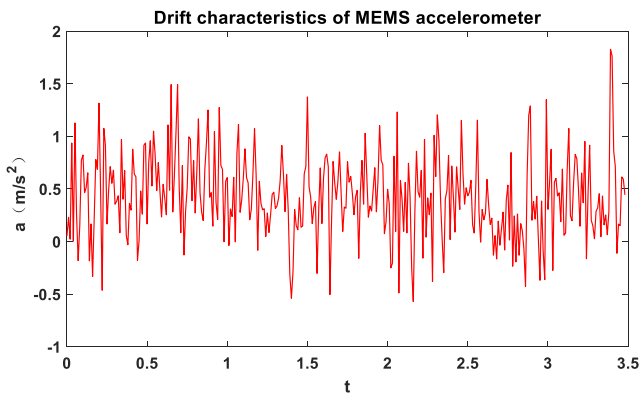


FIG. 7. Random drift characteristics of the MEMS accelerometer.

white Gaussian noises, and their variances are  $Q$  and  $R$ , respectively. First, the state covariance at this time is predicted according to the data value at the moment  $k-1$  as follows:

$$P_{k|k-1} = FP_{k-1}F^T + Q. \quad (10)$$

The Kalman filter gain coefficient at time  $k$  is calculated as follows:

$$K = \frac{P_{k|k-1}H^T}{HP_{k|k-1}H^T + R}. \quad (11)$$

The optimal estimated value at time  $k$  can be obtained using the above formula as follows:

$$X_k = X_{k|k-1} + K(Z_k - HX_{k|k-1}). \quad (12)$$

The covariance at time  $k$  is updated as follows:

$$P_k = (I - KH) P_{k|k-1}. \quad (13)$$

The above steps can be repeated to update the state estimate at each moment so as to achieve the purpose of data optimization. Since there is only one state variable of acceleration signals, the state transition matrices  $A = 1$  and  $H = 1$  in the Kalman filtering formula. The system has no input, so the state control matrix  $B = 0$ . After adjusting the parameter  $Q$  and determining  $R$ , let the initial values  $P_0 = 1$  and  $X_0 = 0$ . The acceleration data can be iteratively optimized. After the Kalman filter algorithm is processed, the random interference signals existing in the acceleration are largely eliminated, as shown in Fig. 8. It can be seen that the Kalman filter algorithm can effectively improve the measurement accuracy of acceleration, which is helpful to improve the calculation accuracy of the distance.

## C. Trend term removal algorithm

In the static state, the sensor also has the fixed output error besides the random output error. This fixed output error is due to the fact that the measurement system is installed in a position and orientation different from the ideal position. In order to study the influence of fixed output error on the distance, it is assumed that the sensor does not have random output error, only fixed output error.

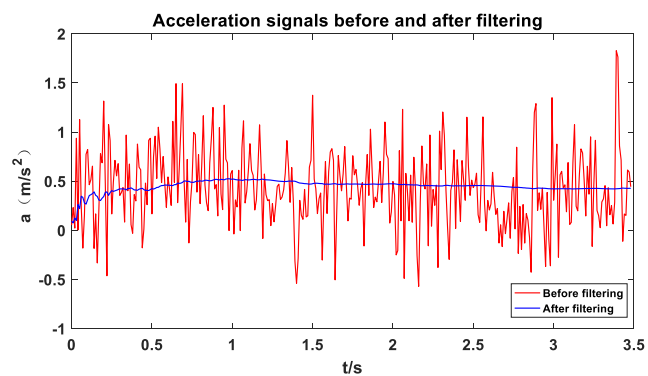


FIG. 8. Comparison of acceleration signals before and after Kalman filtering.

Assume that the size of the fixed output error is  $\xi$ . The actual acceleration of the moving object is  $f(t)$ , and the output of the sensor is  $a(t)$ . Then, there is the following relationship between them:

$$a(t) = f(t) + \xi. \quad (14)$$

Due to the error of sensor output, a serious trend term error will occur in the integration process. The speed and distance of integration will be changed to

$$\begin{aligned} v(t) &= \int_{t_0}^t (a(t) + \xi) dt + v(t_0) \\ &= \int_{t_0}^t a(t) dt + \xi t + \eta + v(t_0), \end{aligned} \quad (15)$$

$$s(t) = \int_{t_0}^t \left( \int_{t_0}^t a(t) dt \right) dt + \frac{1}{2} \xi t^2 + \eta t + v(t_0)t + \delta + s(t_0). \quad (16)$$

In the discrete acceleration integral, the actual velocity and displacement signals are as follows:

$$v[n] = v[n]' + \frac{n}{f} \xi, \quad (17)$$

$$s[n] = s[n]' + \frac{1}{2} \xi \frac{n^2}{f^2}. \quad (18)$$

In the above formula,  $\eta$  is the first order error generated during velocity integration and  $\sigma$  is the first order error generated during displacement integration. As the integration goes on,  $\varepsilon$ ,  $\sigma$ , and  $\eta$  are constantly amplified, and the first trend term error will be generated in the velocity integration, and the second trend term error will be generated in the displacement integration.<sup>21,22</sup> In the discrete domain,  $f$  is the sampling frequency. The continuous accumulation of integration error increases the distance measurement error.

In order to eliminate the effect of the trend term error, suppose that there is a polynomial  $y_m(t)$ ,

$$y_m(t) = \sum_{k=0}^m p_k t^k \in \phi, \quad (19)$$

where  $m$  is the coefficient of the highest degree term,  $P_k$  is a polynomial coefficient, and  $\phi$  is the set of polynomials whose highest degree term does not exceed  $m$ . The trend term error is fitted by the least-squares method as follows:

$$\min = I = \sum_{i=1}^{n-1} [v_i - y_m(t)]^2 = \sum_{i=1}^{n-1} \left[ v_i - \sum_{k=0}^m p_k t_i^k \right]^2. \quad (20)$$

It only needs to determine a set of fitting polynomial coefficients  $P_k$  to get the minimum value of function  $I$ , and then, the optimal trend term fitting result can be obtained. By deriving the multivariate function  $I$ , we can get the following results:

$$\frac{\partial I}{\partial p_j} = 2 \sum_{i=0}^{n-1} \left[ v_i - \sum_{k=0}^m p_k t_i^k \right] t_i^j = 0. \quad (21)$$

A simple expression can be obtained by deformation of the above equation as follows:



FIG. 9. Horizontal slide rail for experiments.

$$\sum_{i=0}^{n-1} v_i t_i^j = \sum_{k=0}^m \left( \sum_{i=0}^{n-1} t_i^{k+j} \right) p_k. \quad (22)$$

After solving the above equation to determine the  $k$  value, the fitting polynomial of the trend term error is also determined. Assume that the sampling frequency of the sensor is  $f_s$ . We can get  $t = i/f_s$  ( $i = 0, 1, 2, \dots, n-1$ ). We can simplify this to a second order matrix. The expression of the coefficient can be obtained by solving the equations as follows:

$$p_0 = \frac{\sum_{i=0}^{n-1} (i/f_s)^2 - \sum_{i=0}^{n-1} (i/f_s) \sum_{i=0}^{n-1} (i/f_s) v_i}{n \sum_{i=0}^{n-1} (i/f_s)^2 - \left[ \sum_{i=0}^{n-1} (i/f_s) \right]^2}, \quad (23)$$

$$p_i = \frac{n \sum_{i=0}^{n-1} (i/f_s) v_i - \sum_{i=0}^{n-1} (i/f_s) \sum_{i=0}^{n-1} v_i}{n \sum_{i=0}^{n-1} (i/f_s)^2 - \left[ \sum_{i=0}^{n-1} (i/f_s) \right]^2}. \quad (24)$$

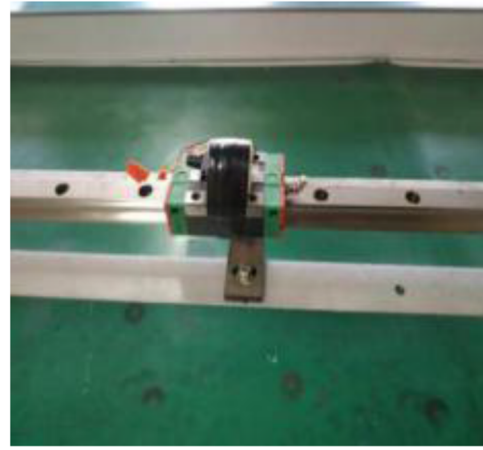


FIG. 10. Installation and fixation of the measuring system.

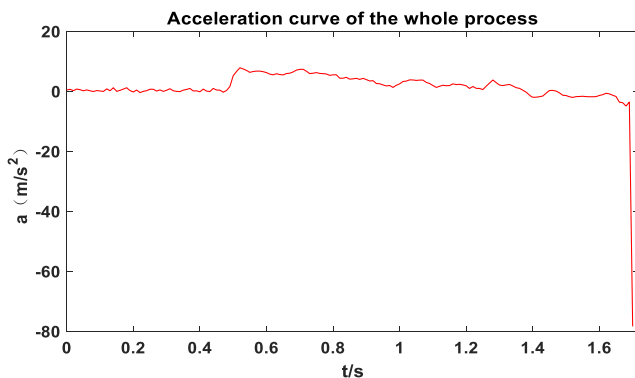


FIG. 11. The acceleration curve of the whole process in the experiment.

The above formula can be used to correct the speed. We can eliminate the trend term of displacement by quadratic term fitting. In addition, displacement can also be corrected based on the velocity signal, and the process is the same.

## V. EXPERIMENTS AND RESULTS

In order to verify the reliability and measurement accuracy of the system, distance measurement tests are carried out. First, the accelerated acquisition program is burned into the DSP through CCS (Code Composer Studio). The test was carried out on a slide track as shown in Fig. 9. The hardware measurement board is packaged with a 3D-printed bracket. The measuring device is fixed to the slider and moves synchronously with the slider as shown in Fig. 10.

First of all, the slider is leveled and marked with the starting position and the end position of the slider. The distance between the start and end is set to 3 m. An obstacle at the end point is placed. When the measuring device is in the initial position, the system switch is turned on and a period of stationary acceleration is collected. The slider then accelerates until it collides with the obstacle at the end. A large acceleration value is the output after the collision between the slider and the obstacle, which marks the end of the test process. The acceleration curve of an experiment is shown in Fig. 11.

It can be seen from the acceleration curve of the whole process that the sensor collects the acceleration in the static state from the initial position. About 0.5 s later, the slider starts to accelerate,

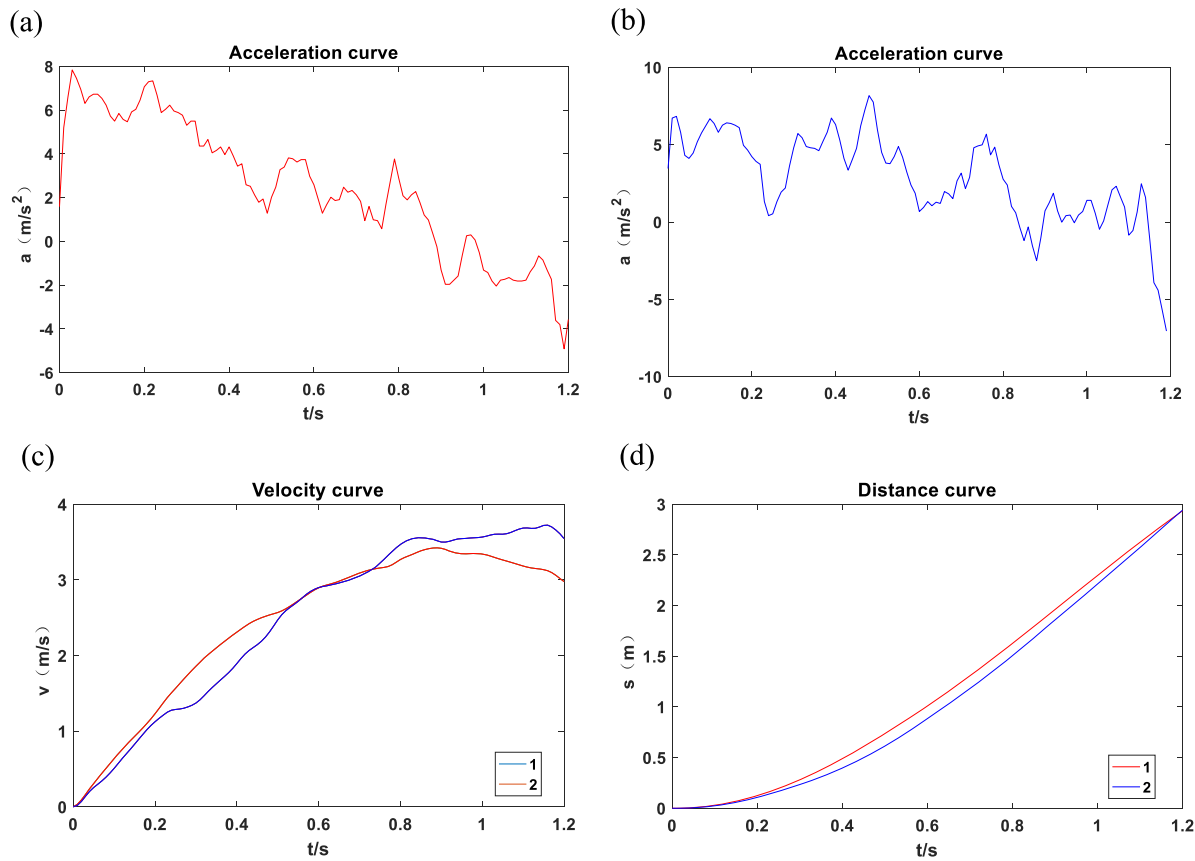


FIG. 12. The curve of acceleration, velocity, and distance over time: (a) acceleration curve 1, (b) acceleration curve 2, (c) real time velocity of the slider in two tests, and (d) real time moving distance of the slider in two tests.

**TABLE II.** Results of five experiments.

No. of tests	Measured distance (m)	Actual distance (m)	Measurement accuracy (%)
1	2.954	3	98.46
2	2.937	3	97.90
3	2.931	3	97.70
4	2.928	3	97.60
5	2.934	3	97.80

and the acceleration changes over time. Until the slider collides with the obstacle, the sensor outputs the maximum acceleration value of  $-78.4 \text{ m/s}^2$ . In order to show the acceleration process more clearly, the sampling point of the sensor in the static state and the maximum acceleration point at the end point were removed. The curves of acceleration, velocity, and distance in two experiments were plotted in MATLAB, as shown in Fig. 12. The distance test results of the five experiments are shown in Table II.

The experimental results verify the feasibility of the measuring system for the distance measurement. The average measurement distance of the five experiments is 2.937 m, and the average measurement accuracy is 97.89%. Due to the random drift and fixed output error of the sensor, the Kalman filter algorithm and the trend error removal algorithm can effectively improve the integration accuracy of the acceleration. Although the installation accuracy and data processing of the measuring system were optimized to the maximum extent during the testing, errors were still unavoidable. On the one hand, the optimized algorithm can only reduce the error to a certain extent, but it cannot completely eliminate the error. On the other hand, the sensor also has a certain output error due to its own accuracy. In addition, the complexity of the motion process and some other uncontrollable factors are also the causes of errors.

## VI. CONCLUSION

This paper has designed a distance measurement system based on the MEMS acceleration sensor. The system takes full advantage of the advantages of small volume, simple interface circuit, and high reliability of the MEMS accelerometer. In this paper, an algorithm is proposed to obtain the distance from the integration of acceleration. The key to obtaining the distance from the integration of acceleration is to obtain the exact acceleration. Effective processing of the acceleration collected using the MEMS accelerometer can improve the accuracy of the data. In this paper, the Kalman filter algorithm and error elimination algorithm are used to improve the accuracy of distance measurement. Because the error characteristics of different types of acceleration sensors are different, the factors affecting measurement accuracy should be fully considered in the design of the measurement system.

The validity and feasibility of the measuring system and its high precision are proved by experiments. The small size of the measuring system can adapt to the flight carrier with narrow internal space. High overload resistance can be used in military and engineering applications, such as aerial target detection and range measurement in complex environments. The next research idea is to continue to optimize the circuit structure to make the system smaller in volume

and lower in power consumption. In addition, the test was carried out in a normal temperature environment, and the influence of temperature on sensor drift was not fully considered. A further study on the effect of temperature on the output of the sensor can enable the measuring system to accurately measure the distance in different environments.

## AUTHORS' CONTRIBUTIONS

All authors contributed equally to this work.

## ACKNOWLEDGMENTS

This work was performed with support and guidance from the Shijiazhuang Municipal Bureau of Science and Technology (Grant No. 2412127).

## DATA AVAILABILITY

The data that support the findings of this study are available from the corresponding author upon reasonable request.

## REFERENCES

- C. Gentile and G. Bernardini, "Output-only modal identification of a reinforced concrete bridge form radar-based measurements," *NDT & E Int.* **41**, 544–553 (2008).
- K.-T. Park, S. H. Kim, H. S. Park *et al.*, "The determination of bridge displacement using measured acceleration," *Eng. Struct.* **27**, 371–378 (2005).
- S.-K. Park, H. W. Park, S. Shin, and H. S. Lee, "Detection of abrupt structural damage induced by an earthquake using time-window technique," *Comput. Struct.* **86**, 1253–1265 (2008).
- G. V. Berg, "Integrated velocity and displacement of strong earthquake ground motion," *Bull. Seismol. Soc. Am.* **51**(2), 175–189 (1961).
- K.-T. Park *et al.*, "The determination of bridge displacement using measured acceleration," *Eng. Struct.* **27**(3), 371–378 (2005).
- D. Hester *et al.*, "Low cost bridge load test: Calculating bridge displacement from acceleration for load assessment calculations," *Eng. Struct.* **143**(15), 358–374 (2017).
- R. Yang *et al.*, "Influence of rain Doppler frequency on MMW Doppler fuze," in *Proceedings of the 9th International Symposium on Antennas, Propagation and EM Theory IEEE* (IEEE, 2011).
- G. Tang, X. Qu, F. Zhang *et al.*, "Absolute distance measurement based on spectral interferometry using femtosecond optical frequency comb," *Opt. Laser Eng.* **120**, 71–78 (2019).
- M. Chen, S. Xie, G. Zhou, D. Wei, H. Wu, S. Takahashi, H. Matsumoto, and K. Takamasu, "Absolute distance measurement based on spectral interferometer using the effect of the FSR of a Fabry–Perot etalon," *Opt. Laser Eng.* **123**, 20–27 (2019).
- W.-m. Niu, F. Li-Qing, Z.-y. Qi *et al.*, "Small displacement measuring system based on MEMS accelerometer accelerometer," *Math. Probl. Eng.* **2019**, 1–7.
- H. S. Lee, Y. H. Hong, and H. W. Park, "Design of an FIR filter for the displacement reconstruction using measured acceleration in low-frequency dominant structures," *Int. J. Numer. Methods Eng.* **82**, 403–434 (2010).
- M. Kumar, S. Yadav, A. Kumar, N. N. Sharma, J. Akhtar, and K. Singh, "MEMS impedance flow cytometry designs for effective manipulation of micro entities in health care applications," *Biosens. Bioelectron.* **142**, 111526 (2019).
- D. Fahimi, O. Mahdavipour, J. Sabino, R. M. White, and I. Paprotny, "Vertically-stacked MEMS PM2.5 sensor for wearable applications," *Sens. Actuators, A* **299**, 111569 (2019).
- I. Marozau, M. Auchlin, V. Pejchal, F. Souchon, D. Vogel, M. Lahti, N. Saillen, and O. Sereda, "Reliability assessment and failure mode analysis of MEMS

- accelerometers for space applications," *Microelectron. Reliab.* **88–90**, 846–854 (2018).
- <sup>15</sup>F. Mohd-Yasin, C. E. Korman, and D. J. Nagel, "Measurement of noise characteristics of MEMS accelerometers," *Solid-State Electron.* **47**, 357–360 (2003).
- <sup>16</sup>L. Feng, W. Gu, K. Zhao *et al.*, "Novel self-compensation method to lower the temperature drift of a quartz MEMS gyroscope," *Microsyst. Technol.* **20**, 2231–2237 (2014).
- <sup>17</sup>M. Park and Y. Gao, "Error analysis and stochastic modeling of low-cost MEMS accelerometer," *J. Intell. Rob. Syst.* **46**, 27–41 (2006).
- <sup>18</sup>E. Song *et al.*, "Optimal Kalman filtering fusion with cross-correlated sensor noises," *Automatica* **43**, 1450–1456 (2007).
- <sup>19</sup>R. Antonello *et al.*, "Acceleration measurement drift rejection in motion control systems by augmented-state kinematic Kalman filter," *IEEE Trans. Ind. Electron.* **63**, 1953 (2016).
- <sup>20</sup>Y. Wu *et al.*, "Dynamic magnetometer calibration and alignment to inertial sensors by Kalman filtering," *IEEE Trans. Control Syst. Technol.* **26**, 716 (2017).
- <sup>21</sup>S. C. Stiros, "Errors in velocities and displacements deduced from accelerographs: An approach based on the theory of error propagation," *Soil Dyn. Earthquake Eng.* **28**(5), 415–420 (2008).
- <sup>22</sup>H. H. Yun, H. K. Kim, and H. S. Lee, "Reconstruction of dynamic displacement and velocity from measured accelerations using the variational statement of an inverse problem," *J. Sound Vib.* **329**(23), 4980–5003 (2010).